

Budding Dynamics of Multicomponent Tubular Vesicles

Li Li, Xinyu Liang, Meiyu Lin, Feng Qiu,* and Yuliang Yang*

The Key Laboratory of Molecular Engineering of Polymers, Ministry of Education, Department of Macromolecular Science, Fudan University, Shanghai 200433, China

Received October 2, 2005; E-mail: fengqiu@fudan.edu.cn; ylyang@srcap.stc.sh.cn

Multicomponent lipid vesicles are widely used as model systems of cell membranes to mimic many important life activities, such as the intracellular signaling and the movement of biochemical cargoes within and between the cells.^{1,2} Domain or bud formation in multicomponent membranes and their further spontaneous protrusion compose the first step of the delivery of proteins, carbohydrates, or lipids in the cells.^{3,4} Previous studies have focused on the influences of the composition and temperature on the coexisting domain patterns.^{5,6} Typical equilibrium thermodynamic phase diagrams of model membranes composed of phosphatidylcholines and cholesterol were constructed.^{7,8} The correlations between the vesicle composition and the local membrane curvature were investigated, although there was only static shape information available due to the limitation of the imaging speed of two-photon fluorescence microscopy.⁹ Recently, a spatio-temporal evolution of periodic superstructures in phase-separated, flat membranes has been described.¹⁰ Until now, the dynamic aspect of the bud formation was only probed by computer simulations.^{11–15} Our experiments, by choosing tubular shape vesicles and suitable fluorescence microscopy, have successfully captured the real-time budding dynamics and showed a difference between the diffusivity of the buds on the lipid membrane and that of the embedded cell membrane proteins.

Due to the constraint of both the area and encapsulated volume, when a spherical multicomponent vesicle in equilibrium is cooled, only weakly curved domains can form on such a membrane. This has made observing the real-time budding process difficult. Here we show that making vesicles with a large area-to-volume ratio, such as tubular vesicles, which allow enough number of buds to pinch off from the phase-separated membrane, is a precondition for real-time dynamic investigations.

We used the method of direct-hydration-swelling in situ to prepare the vesicles.⁷ Equimolar 1,2-dioleoyl-*sn*-glycero-3-phosphocholine (DOPC), 1,2-dipalmitoyl-*sn*-glycerol-3-phosphocholine (DPPC), and cholesterol (Chol) were dissolved in chloroform/methanol (9:1 by volume) to 1.9 mg/mL. Texas Red 1,2-dihexadecanoyl-*sn*-glycerol-3-phosphoethanolamine (Texas Red DHPE) was chosen as the dye for contrast at a concentration of 0.3 wt % (TR DHPE/lipid). A 3 μ L droplet of such lipid solution (stored at -20 °C) was deposited on the center of a prewarmed glass slice and then kept in vacuum at 50 °C for overnight. The glass slice with dry lipid film was moved from vacuum and placed on a 50 °C heating stage (THMS600, Linkam, England) under a fluorescence microscope (BX51, Olympus, Japan) equipped with a 50 \times semi-achroplane objective (NA = 0.5). Tiny water drops (2 μ L) were put on the film two times for prehydration, followed by a large water droplet (around 20 μ L) to cover the film for hydration and incubation, a variety of shapes of unilamellar and multilamellar vesicles formed and grew up in the incubated solvent. Then the sample was quenched to 20 °C (which was below the miscibility temperature of the ternary mixture⁵) at a rate of 8 °C/min, and the

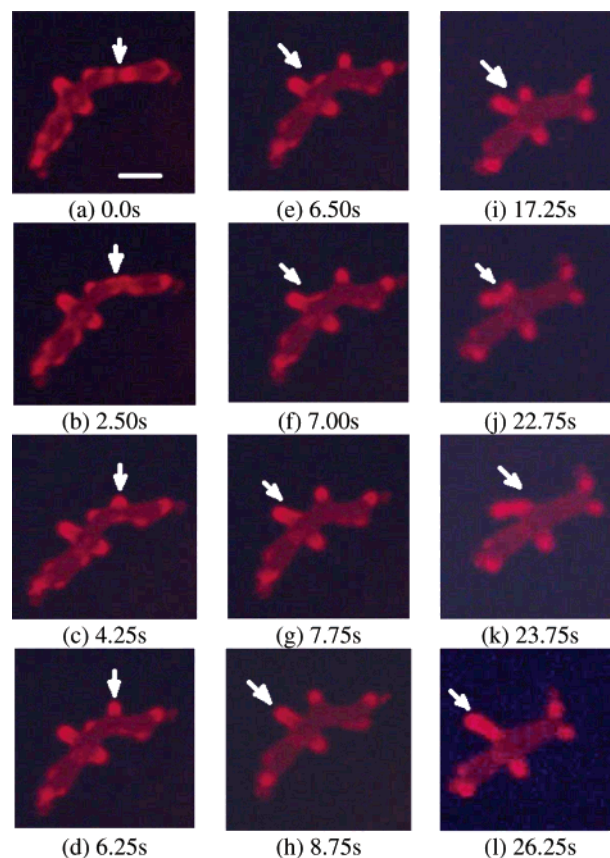


Figure 1. Three typical growth modes for the budding process. (a–d) Growth mode I, (e–h) growth mode II, and (i–l) growth mode III. The scale bar corresponds to 10 μ m.

phase separation was triggered, in which DPPC and cholesterol enriched into a liquid phase with short-range order, while DOPC preferred a disordered liquid phase. The Texas Red DHPE preferentially partitioned into the cholesterol-poor DOPC phase. Choosing transparent tubular vesicles with a large length-to-radius ratio as the candidate, the budding processes were recorded with a fixed focal plane at a rate of 2 or 4 frames/s by a CCD camera (Pixelink, Linkam, England). The images were two-dimensional and analyzed by Linksys32DV (Linkam, England) and SPOT Advanced (Diagnostic Ins, USA) software.

Three typical growth modes in the budding process are shown in Figure 1. Growth mode I (Figure 1a–d) is the formation of a single bud through the coalescence between flat patches. In this mode, a patch enriched with DOPC is observed to form at first, followed by its growth toward the outer surface of the vesicle.

The growth mode II involves the coalescence of a bud and a patch (Figure 1e–h), in which the patch merges into the root of the bud and causes the bud to lean toward the opposite direction. After the coalescence, the bud bounces back to be perpendicular

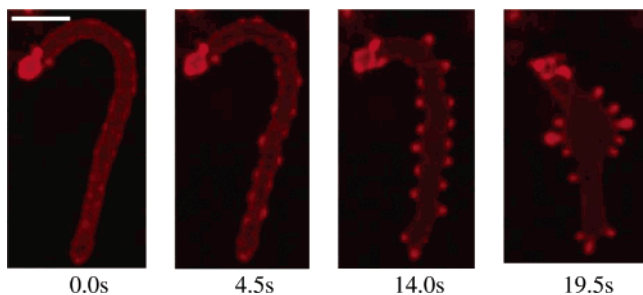


Figure 2. Budding process of a tubular vesicle. The scale bar corresponds to 10 μm .

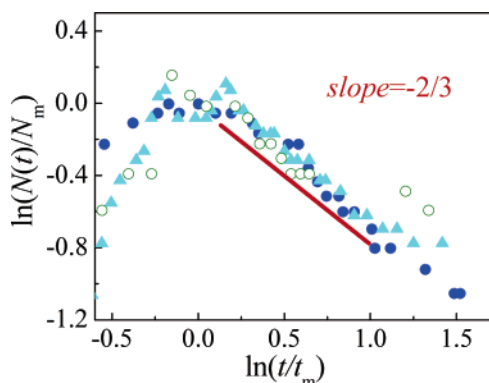


Figure 3. Double-logarithmic plot for the number of buds on the vesicles as a function of time. Data obtained from three different tubular vesicles (corresponding to dot, circle, and triangle, respectively) are shown. Each set of data is rescaled by N_m and t_m , in which N_m (in a range of 14–29) is the peak value of the bud number obtained by parabola fitting, and t_m is the time at which N_m is reached. The slope of the line is $-2/3$.

to the tubular; the time of the coarsening is about 2 s, and the bouncing back takes almost the same time. The time scale of the bouncing back can be used to estimate the bending rigidity of the membrane. The typical relaxation time, t_r , for the membrane undulation can be calculated by standard hydrodynamic mode analysis as $t_r \sim \eta L^3/\kappa$, where η is the dynamic viscosity of the solvent (water in this case) and κ is the bending rigidity of the membrane.¹⁶ Using the typical values $t_r \sim 1$ s, $\eta \sim 10^{-3}$ Pa·s, and $L \sim 5$ μm , κ is estimated to be $\sim 10^{-19}$ J, which is in agreement with the typical value measured for phospholipids. Growth mode III describes the coalescence of two buds (Figure 1i–l). We note that in this process, as their roots start to merge together, both of the two buds lean oppositely toward the vesicle surface due to the bending elasticity of the membrane, forming a “V” shape. After a few seconds (~ 2 s), the shorter branch of the V diminishes and then the longer branch bounces back.

Figure 2 shows the shape evolution of a typical tubular vesicle during the budding process. The number of the buds on the contour line of the tubes is counted with the help of the software mentioned previously. Statistically, this number is proportional to the total number of the buds on the whole vesicle surface since the focal plane was fixed. Figure 3 is the statistical result of the time dependence of the bud number, N . Six independent examples were successfully captured. For clarity, only three of them, which have larger N_m and longer time of evolution, are shown. Initially, the number of the buds increases because growth mode I dominates. As the budding process proceeds, there is a short stage, in which the three modes are balanced. After that, the bud coarsening (mode

III) dominates, and N decays monotonically with time, following a scaling law $N \sim t^{-\beta}$, with $\beta \sim 2/3$, which confirms the recent prediction by Dissipative Particle Dynamics simulation.¹⁵ The 2/3 exponent can be understood by the scaling argument following ref 15. Since the total areas A_o occupied by DOPC and A_p by DPPC and cholesterol are constant in the budding process, one has $N \sim A_o/R^2(t)$ and $l(t) \sim (A_p/N)^{1/2}$, thus $l(t) \sim R(t)$, where $R(t)$ and $l(t)$ denote the domain size and the average distance between the two domains at time t , respectively. In this stage, the domain growth occurs mainly through the coalescence of buds themselves or flat patches with buds (which is rare); however, before the two domains can coalesce, they must diffuse by a distance on the order of l . If one assumes the Stokes–Einstein relation, that is, $D \sim k_B T/\eta R$, with D being the diffusion constant, then the corresponding diffusion time t is given by $t \sim l^2/D \sim R^3$. Therefore, one has $R \sim t^{1/3}$, and the bud number decays as $N \sim t^{-2/3}$.

We believe that the results presented here do not depend on the specific dye we used. In fact, Texas Red DHPE, Rhodamine-DPPE, and Perylene have been extensively used to study the phase separation of various multicomponent lipid vesicles.^{5,7,9,10} We also note that for a 2D fluid membrane, the diffusivity of the embedded particles, such as integral cell membrane proteins, depends only weakly on their size,¹⁷ leading to $R \sim t^{1/2}$ and $N \sim t^{-1}$. This, however, contradicts the observed scaling exponent in the present experiment. We attribute this discrepancy to the fact that the main body of the bud is actually immersed in the surrounding aqueous phase and cannot be treated as a purely 2D structure any more. In fact, the buds diffuse much slower than the integral membrane proteins.

In summary, we have identified three typical growth modes of the budding process in multiphase tubular vesicles by employing fluorescence microscopy. In particular, we found that the bud number decayed with time in the late stage of budding, following a scaling form as $N \sim t^{-\beta}$, with $\beta = 2/3$. Our observation showed a difference between the diffusivity of the buds on the lipid membrane and that of the embedded membrane proteins.

Acknowledgment. This work was supported by the National Natural Science Foundation of China.

References

- (1) Binder, W. H.; Barragan, V.; Menger, F. M. *Angew. Chem., Int. Ed.* **2003**, *42*, 5802–5827.
- (2) Lipowky, R.; Dimova, R. *J. Phys.: Condens. Matter.* **2003**, *15*, s31–s45.
- (3) Brown, D. A.; London, E. *Annu. Rev. Cell Dev. Biol.* **1998**, *14*, 111–136.
- (4) Lippincott-Schwartz, J.; Roberts, T. H. *Annu. Rev. Cell Dev. Biol.* **2000**, *16*, 557–589.
- (5) Veatch, S. L.; Keller, S. L. *Phys. Rev. Lett.* **2002**, *89*, 268101–1–4.
- (6) Feigensohn, G. W.; Buboltz, J. T. *Biophys. J.* **2001**, *80*, 2775–2788.
- (7) Veatch, S. L.; Keller, S. L. *Biophys. J.* **2003**, *85*, 3074–3083.
- (8) de Almeida, R. F. M.; Fedorov, A.; Prieto, M. *Biophys. J.* **2003**, *85*, 2406–2416.
- (9) Baumgart, T.; Hess, S. T.; Webb, W. W. *Nature* **2003**, *425*, 821–824.
- (10) Rozovsky, S.; Kaizuka, Y.; Groves, J. T. *J. Am. Chem. Soc.* **2005**, *127*, 36–37.
- (11) Kumar, P. B. S.; Rao, M. *Mol. Cryst. Liq. Cryst.* **1996**, *288*, 105–118.
- (12) Kumar, P. B. S.; Rao, M. *Phys. Rev. Lett.* **1998**, *80*, 2489–2492.
- (13) Taniguchi, T. *Phys. Rev. Lett.* **1996**, *76*, 4444–4447.
- (14) Kumar, P. B. S.; Gompper, G.; Lipowsky, R. *Phys. Rev. Lett.* **2001**, *86*, 3911–3914.
- (15) Laradji, M.; Kumar, P. B. S. *Phys. Rev. Lett.* **2004**, *93*, 198105–1–4.
- (16) Zilman, A. G.; Granek, R. *Phys. Rev. Lett.* **1996**, *77*, 4788–4791.
- (17) Saffman, P. G.; Delbrück, M. *Proc. Natl. Acad. Sci. U.S.A.* **1975**, *72*, 3111–3113.

JA0567438